Degenerative Neurological and Neuromuscular Disease

Dovepress
Taylor & Francis Group

Open Access Full Text Article

ORIGINAL RESEARCH

Proteomic Identification of ALDOA as a Pathogenic TDP-43 Interaction Partner in ALS

Kaixin Yan[1,*], Jinfeng Deng[2,*], Yuxuan Yong[1], Fangfang Bi[1,2]

[1]Department of Neurology, Second Affiliated Hospital of Xinjiang Medical University, Urumqi, Xinjiang Uyghur Autonomous Region, People's Republic of China; [2]Department of Neurology, The Fifth Affiliated Hospital of Sun Yat-Sen University, Zhuhai, Guangdong, People's Republic of China

*These authors contributed equally to this work

Correspondence: Fangfang Bi, Department of Neurology, The Fifth Affiliated Hospital of Sun Yat-sen University, Zhuhai, Guangdong, People's Republic of China, Email biff3@mail.sysu.edu.cn; Yuxuan Yong, Department of Neurology, Second Affiliated Hospital of Xinjiang Medical University, Urumqi, Xinjiang Uyghur Autonomous Region, People's Republic of China, Email yongyuxuan@126.com

Objective: Amyotrophic lateral sclerosis (ALS) is a fatal neurodegenerative disease affecting both upper and lower motor neurons, and its pathogenesis has not been fully elucidated. TAR DNA-binding protein 43 (TDP-43), as one of the key pathogenic genes in ALS, participates in the disease process through interactions with various proteins. This study aims to investigate the interaction mechanism between TDP-43 and aldolase A (ALDOA) in ALS.

Methods: HEK293T cell models transfected with wild-type and mutant TDP-43 (TDP-43^{M337V}) plasmids were constructed. The interaction between TDP-43 and ALDOA was analyzed through proteomic screening of specific peptides and co-immunoprecipitation, and the co-localization of the two in cells was detected by immunofluorescence. Changes in ALDOA expression levels after intervention with mutant TDP-43 were detected by Western blot and quantitative real-time PCR.

Results: Proteomic analysis identified ALDOA as a potential interacting protein of TDP-43. Protein-protein interaction (PPI) analysis, co-immunoprecipitation, and immunofluorescence experiments further confirmed that both wild-type and mutant TDP-43 interact with ALDOA. Western blot and quantitative real-time PCR results showed that, compared with the wild-type TDP-43 group, the ALDOA expression was significantly increased in the TDP-43^{M337V} mutant group.

Conclusion: TDP-43 interacts with ALDOA in ALS, and the TDP-43^{M337V} mutation significantly promotes ALDOA expression, suggesting that ALDOA may be involved in the pathogenesis of TDP-43-mediated ALS. These findings provide new insights into the pathogenesis of ALS and highlight a potential therapeutic target.

Keywords: TDP-43, ALDOA, amyotrophic lateral sclerosis, proteomics, neurodegenerative diseases

Introduction

Amyotrophic lateral sclerosis (ALS) is a chronic progressive neurodegenerative disease that primarily affects the upper and lower motor neurons.[1] Patients often initially present with progressively worsening muscle weakness and atrophy. As the disease advances, it gradually involves the muscles responsible for swallowing, speech, and respiration. In the late stages, widespread muscle atrophy becomes pronounced, leading to dysphagia and respiratory muscle paralysis, with the majority of patients ultimately succumbing to respiratory failure.[2] Research suggests that multiple mechanisms collectively contribute to the pathogenesis of ALS, including oxidative stress, excitotoxicity, mitochondrial and proteasomal dysfunction, abnormal RNA metabolism, impaired axonal transport, and neuroinflammation.[3] Currently, Riluzole and Edaravone are the only drugs approved by the FDA for ALS treatment; however, they can only partially alleviate symptoms and marginally extend patient survival, without halting or reversing disease progression.[4] Although emerging strategies like gene therapy offer new directions for ALS treatment,[5] they remain largely exploratory, and effective therapeutic targets and interventions for the disease are still scarce.

The TAR DNA-binding Protein of 43 kDa (TDP-43) is a key pathological hallmark in various neurodegenerative diseases, including ALS.[6,7] Abnormal, ubiquitinated, and phosphorylated TDP-43 inclusions are found in the affected

Received: 22 April 2025
Accepted: 20 November 2025
Published: 7 December 2025

neurons of approximately 97% of ALS patients and a significant subset of patients with Frontotemporal Lobar Degeneration (FTLD).[8,9] The core pathogenic mechanisms of TDP-43 involve a loss of its nuclear function, leading to dysregulation of RNA metabolism,[10] and the abnormal aggregation of its C-terminal domain in the cytoplasm, forming neurotoxic amyloid aggregates. In familial ALS, various C-terminal mutations disrupt protein homeostasis,[11] causing multiple cellular functional defects and activating degradation pathways, thereby creating a vicious cycle.[12]

ALDOA, a member of the aldolase family, plays a crucial role in glycolysis and gluconeogenesis by reversibly catalyzing the conversion of fructose-1,6-bisphosphate to glyceraldehyde-3-phosphate and dihydroxyacetone phosphate.[13] Dysregulation of its expression can mediate glycolytic dysfunction. Previous studies have indicated that enhanced glycolysis promotes the progression of neurodegenerative diseases such as Parkinson's disease (PD).[14,15] A proteomic analysis of cerebrospinal fluid from AD patients revealed a significant increase in ALDOA expression levels.[16] However, the interaction between TDP-43 and ALDOA remains to be elucidated. Meanwhile, the impact of TDP-43 gene mutations on ALDOA function in the context of ALS requires further investigated.

Proteomics is a discipline focused on the study of the proteome, dedicated to the systematic analysis of protein expression levels, post-translational modification states, and protein-protein interaction networks, thereby comprehensively revealing the overall molecular mechanisms of disease pathogenesis and cellular metabolic regulation.[17] This technology has been widely applied in the field of neurodegenerative disease research, playing a significant role in screening disease-related biomarkers and providing in-depth insights into pathogenic molecular mechanisms.[18,19] This study comprehensively utilizes proteomic analysis and molecular biology experiments to screen proteins interacting with TDP-43 and construct their interaction network. It further validates changes in ALDOA expression levels to deeply explore the interaction between TDP-43 and ALDOA and its potential mechanism in ALS. The aim is to provide new theoretical foundations and potential therapeutic targets for ALS pathological mechanism research and clinical treatment.

Materials and Methods

Materials

The HEK-293T cell line was purchased from Procell Life Science & Technology Co., Ltd. Fetal bovine serum (FBS) was obtained from Lonsera (S711-001S, China). Lipofectamine™ 3000 Transfection Reagent was provided by Thermo Fisher Scientific (L3000015, USA). Opti-MEM™ I Reduced Serum Medium was purchased from Thermo Fisher Scientific (31985070, USA). The BCA Protein Assay Kit was acquired from Solarbio (PC0020, China).

Cell Culture

All cells were cultured and preserved at the Fifth Affiliated Hospital of Sun Yat-sen University. HEK-293T cells were maintained in DMEM medium (GIBCO, USA) supplemented with 10% fetal bovine serum and 1% penicillin/streptomycin. For cell resuscitation, cryovials were retrieved from liquid nitrogen and quickly placed in a 37°C water bath with gentle shaking until thawed. After complete thawing, the cell suspension was transferred to a centrifuge tube, mixed with an appropriate amount of complete medium, and subjected to low-speed centrifugation followed by supernatant removal. The cells were then seeded in DMEM medium (GIBCO, USA) containing 10% fetal bovine serum and 1% penicillin/streptomycin, and incubated at 37°C in a 5% CO_2 incubator. Cells beyond the 20th passage were excluded from the experiments.

Cell Transfection

HEK293T cells at 60% confluence were transfected with the following plasmids: Vector (GL107 pSLenti-EF1-EGFP-P2A-Puro-CMV-MCS-3×FLAG-WPRE), Flag-TDP-43 (pSLenti-EF1-EGFP-P2A-Puro-CMV-Tardbp(Tdp43)-3×FLAG-WPRE), and Flag-TDP-43 M337V (pSLenti-EF1-EGFP-P2A-Puro-CMV-Tardbp(p.M337V)-3×FLAG-WPRE). For each transfection, 3 μg of plasmid was diluted in 200 μL of Opti-MEM™ I Reduced Serum Medium and incubated for 5 minutes. Separately, 6 μL of Lipofectamine™ 3000 transfection reagent was mixed with 200 μL of Opti-MEM™ I Reduced Serum Medium and also incubated for 5 minutes. The two solutions were then combined, mixed gently, and

further incubated for 5 minutes. The resulting mixture was added to the respective cell groups, and cells were harvested 48 hours post-transfection.

Sample Preparation

Proteins were extracted from the cells using a mixture of protein lysis buffer and protease inhibitors. After lysis and centrifugation, the supernatant was collected. Protein concentration was determined using the BCA Protein Assay Kit to ensure consistency across groups in subsequent experiments. Input samples were prepared as controls, and co-immunoprecipitation (IP) samples were prepared to enrich proteins interacting with TDP-43.

Mass Spectrometry Analysis and Screening

Peptides were dissolved in mobile phase A and separated using an EASY-nLC 1200 ultra-high-performance liquid chromatography (UHPLC) system. Mobile phase A consisted of aqueous solution containing 0.1% formic acid and 2% acetonitrile; mobile phase B consisted of aqueous solution containing 0.1% formic acid and 90% acetonitrile. The liquid chromatography gradient was set as follows: 0–14.5 min, 6%–22% B; 14.5–17.5 min, 22%–34% B; 17.5–19 min, 34%–80% B; 19–20 min, 80% B, with a flow rate maintained at 700 nl/min.

After separation by the UHPLC system, the peptides were ionized via an NSI ion source and then analyzed using an Orbitrap Exploris 480 mass spectrometer. The ion source voltage was set to 2300 V, and the FAIMS compensation voltage (CV) was set to −45 V. Both the precursor ions and their secondary fragments were detected and analyzed using the high-resolution Orbitrap. The primary mass spectrometry scanning range was set to 350–1400 m/z with a resolution of 60,000; the secondary mass spectrometry scanning range started fixed at 120 m/z with a resolution of 15,000.

Data acquisition was performed using data-independent acquisition (DIA), where after full MS^1 scanning, peptide ions within multiple consecutive m/z windows were fragmented in the HCD collision cell with 27% fragmentation energy, followed by sequential MS^2 analysis. To improve mass spectrometry efficiency, the automatic gain control (AGC) was set to 1E6 and the maximum injection time was set to 22 ms.

Bioinformatics Analysis

The database accession numbers or protein sequences of differentially expressed proteins identified from comparative groups were compared against the STRING protein-protein interaction database. Interactions with a confidence score > 0.7 (high confidence) were extracted to construct the protein interaction network of differentially expressed proteins. The network was then visualized using the R package "visNetwork".

Co-Immunoprecipitation Assay

First, collect the cells to be analyzed and lyse them on ice using a pre-cooled RIPA lysis buffer for 30 minutes. Then, centrifuge the lysate at 4°C and 12,000 × g for 15 minutes to remove cell debris. The resulting supernatant, referred to as Supernatant A, contains the total protein extract, and its concentration should be determined.

Next, divide Supernatant A equally into two portions: one for the experimental group, to which a specific antibody against the target protein is added, and the other for the negative control group, to which the same amount of a non-specific immunoglobulin from the same species or IgG is added. Incubate the mixtures overnight at 4°C with slow agitation to allow sufficient formation of immune complexes between the antibodies and the target protein.

The following day, add an appropriate amount of Protein A/G magnetic beads, pre-washed with lysis buffer, to each reaction system. Continue incubation at 4°C with slow agitation for 2–4 hours to efficiently capture the antibody-target protein complexes by the magnetic beads.

After incubation, place the samples on a magnetic stand and discard the supernatant. Wash the precipitated magnetic beads 3–4 times with pre-cooled lysis buffer to thoroughly remove non-specifically bound proteins.

Finally, add an appropriate volume of 1× SDS-PAGE loading buffer to the magnetic bead pellet, heat the mixture at boiling temperature for 5–10 minutes, and then collect the supernatant by centrifugation for subsequent Western Blotting analysis.

Western Blot

SDS-PAGE gels with concentrations ranging from 6% to 12% were prepared. Samples were loaded at 30 μg of protein per well. Electrophoresis was performed at a constant voltage of 100 V to separate the proteins, which were then transferred to a PVDF membrane under a constant current of 400 mA. The membrane was subsequently blocked with TBST containing 5% skim milk at room temperature for 1 hour.

After blocking, the membrane was incubated overnight at 4 °C with the following primary antibodies: anti-ALDOA (1:1000, 11,217-1-AP, Proteintech, China), anti-TDP-43 (1:1000, 10,782-2-AP, Proteintech, China), and anti-Tubulin (1:5000, 11,224-1-AP, Proteintech, China). The membrane was then washed three times with TBST to remove unbound primary antibodies.

Next, corresponding species-specific HRP-conjugated secondary antibodies (1:5000) were applied and incubated at room temperature for 1 hour. After incubation, the membrane was washed again with TBST. Finally, specific protein bands were detected using a chemiluminescence imaging system, and band intensity was quantified to compare the expression levels of target proteins across different samples.

Immunofluorescence

After removing the culture medium, HEK293T cells were gently washed twice with room temperature PBS buffer for 5 seconds each. Then, 4% neutral formaldehyde fixative was added to cover the cells and incubated at room temperature for 15 minutes. After fixation, the fixative was discarded, and the cells were washed three times with pre-chilled PBS buffer (4°C) for 5 minutes each. Subsequently, the cells were permeabilized with Triton X-100 on ice for 10 minutes.

After permeabilization, the samples were covered with 5% goat serum and blocked at room temperature for 1 hour. The blocking solution was then removed, and the samples were incubated overnight at 4°C with the following primary antibodies: anti-ALDOA (1:200 dilution, Cat# ab252953, Abcam, USA) and anti-TDP-43 (1:200 dilution, Cat# 10782-2-AP, Proteintech, Wuhan, China).

The next day, the primary antibodies were discarded, and species-specific HRP-conjugated secondary antibodies were applied to cover the samples. Incubation was carried out at room temperature for 2 hours in the dark. The samples were then washed three times with PBS buffer. Finally, an anti-fade mounting medium was applied, and the images were observed and captured under a fluorescence microscope.

Statistical Analysis

Data from in vivo experiments were analyzed using GraphPad Prism 10.3.1 and the statsmodels Python package (v0.13.0). An unpaired *t*-test was employed for comparisons. All data presented as mean ± SD. Statistical significance was set at $P < 0.05$.

Results

Construction of TDP-43 Wild-Type and TDP-43 Mutant Cell Models

Forty-eight hours after plasmid transfection into HEK293T cells from each group, transfection efficiency was observed under a fluorescence microscope. The results showed a high fluorescence expression rate in each group, indicating successful plasmid transfection (Figure 1A). Silver staining results revealed clear protein bands in the silver-stained profiles of all samples, demonstrating good integrity and effective separation of the protein samples. Under equal protein concentrations, differences in protein expression patterns were observed among the groups, suggesting that plasmid transfection led to alterations in the protein expression profiles (Figure 1B).

Proteomic Analysis Reveals an Interaction Between ALDOA and TDP-43

Based on the mass spectrometry results, we successfully identified a specific peptide sequence of the ALDOA protein using affinity purification coupled with mass spectrometry. In the MS/MS spectrum of this peptide, we observed continuously distributed b-ions (b2–b4, b8–b11) and y-ions (y3, y7–y12) fragment signals. The most abundant fragment ions included y10+ (m/z 1049.51), y11+ (m/z 907.44), and y12+ (m/z 1162.6), while characteristic ions such as b3+ (m/z

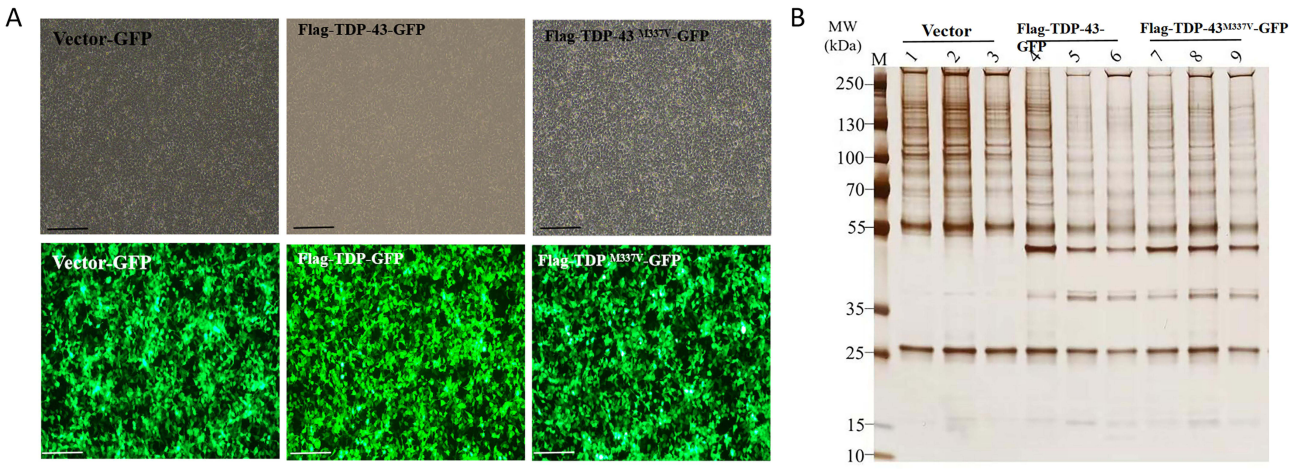

Figure 1 Successful plasmid transfection in HEK293T cells and qualified protein samples. (**A**) Fluorescence microscopy images showing transfection efficiency in each group of cells (200×, n=3); (**B**) Silver staining results (n=3).

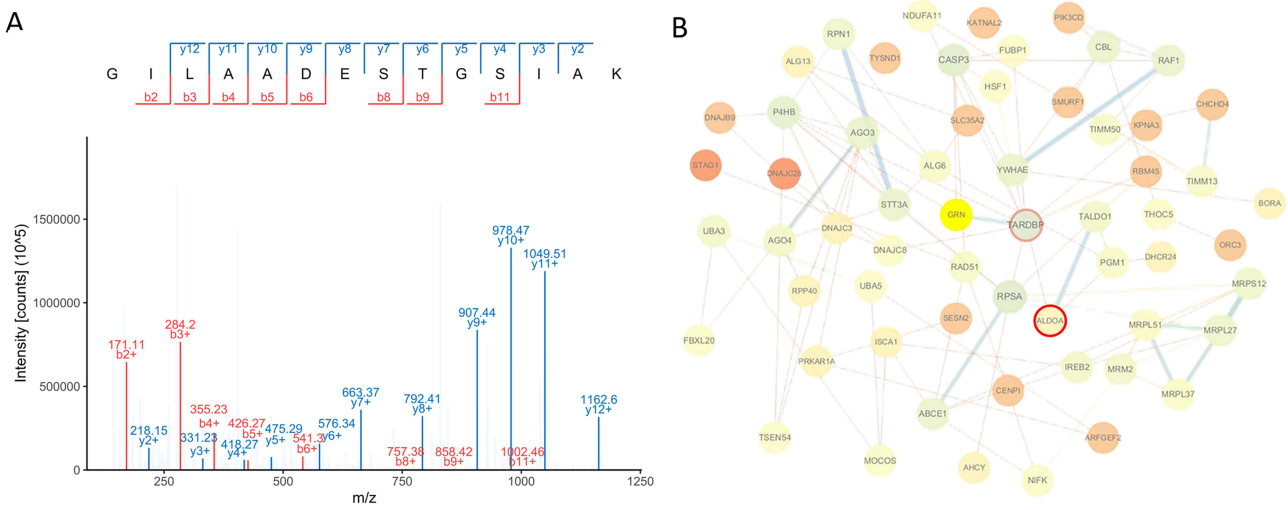

Figure 2 Proteomic analysis reveals an interaction between ALDOA and TDP-43. (**A**) Mass spectrometry identification of a specific peptide derived from ALDOA; (**B**) Protein-protein interaction (PPI) network. TARDBP (TDP-43) and its interaction partner ALDOA are highlighted by red circles.

284.2) and b4+ (m/z 355.23) were also detected in the low-mass region. These complementary ion series provided comprehensive fragment coverage, confirming that the peptide sequence is GAA DESGSK, corresponding to residues 120–128 of the ALDOA protein, which confirms the definite expression of ALDOA in the sample (Figure 2A).

By comparing results with the STRING protein-protein interaction database and extracting interactions with a confidence score > 0.7 (high confidence), differential protein interaction relationships were obtained. Using Cytoscape software, a differential protein interaction network including ALDOA was constructed. The network analysis revealed that ALDOA occupies a central position and exhibits an interaction with TDP-43 (Figure 2B).

Validation of the Interaction and Co-Localization Between TDP-43 and ALDOA in HEK293T Cells

In this study, the expression and localization of TDP-43 and ALDOA within cells were detected by immunofluorescence assays. Following plasmid transfection, TDP-43 was localized to both the nucleus and cytoplasm, whereas ALDOA was predominantly nuclear. Consequently, the co-localization of the two proteins was primarily observed in the nucleus (Figure 3A and B). Furthermore, to further validate the interaction between the two proteins, we performed co-

https://doi.org/10.2147/DNND.S535954

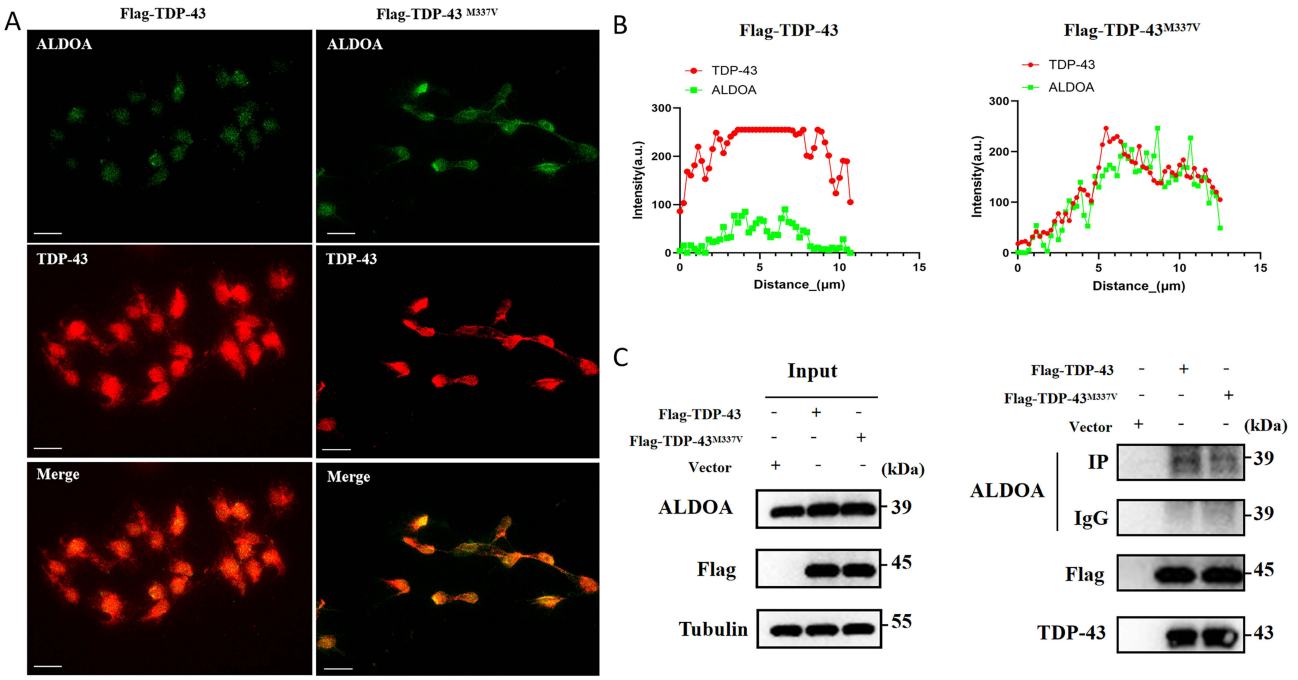

Figure 3 Interaction between ALDOA and TDP-43 validated by immunofluorescence and co-immunoprecipitation. (**A**) Immunofluorescence images showing co-localization of ALDOA (green) and TDP-43 (red) in each group of cells; Bar = 50 μm. (**B**) Visual representation of fluorescence co-localization from (**A**). (**C**) Western blot results of co-immunoprecipitation assays.

immunoprecipitation experiments. The results indicated that no ALDOA signal was detected in the Vector control group, whereas distinct ALDOA bands were observed in both the wild-type and mutant TDP-43 groups (Figure 3C), suggesting that ALDOA interacts directly or indirectly with both wild-type and mutant TDP-43.

TDP-43 Gene Mutation Leads to Upregulation of ALDOA Expression in HEK293T Cells

Western blot results further confirmed that TDP-43 protein bands were effectively detected in both the Vector control group and the mutant TDP-43 transfection group, with the TDP-43 protein expression level in the mutant TDP-43 transfection group being significantly higher than that in the Vector control group, indicating successful plasmid transfection (Figure 4A and B, $P < 0.0001$). Concurrently, at the protein level, ALDOA expression was significantly upregulated in the mutant TDP-43 transfection group compared to the Vector group (Figure 4A and C, $P = 0.0157$). Quantitative real-time PCR results showed that ALDOA mRNA expression was significantly higher in the mutant TDP-43 transfection group than in the Vector group (Figure 4A and D, $P = 0.0117$).

Discussion

Amyotrophic lateral sclerosis (ALS) is a highly debilitating motor neuron disease for which no effective treatment is currently available.[4] The pathogenesis of ALS involves multiple mechanisms, including oxidative stress, mitochondrial and proteasomal dysfunction, abnormal RNA metabolism, altered synaptic function, disrupted axonal transport, and neuroinflammation.[20] Previous studies have identified the pathological roles of certain brain proteins in ALS progression, such as TDP-43[21] and FUS,[22] whose mutations or dysfunctions can trigger various neurodegenerative diseases.[23,24]

TDP-43, encoded by the TARDBP gene, is a highly conserved nuclear protein primarily localized in the nucleus. It plays a critical role in regulating RNA transcription, alternative splicing, and the processing of miRNAs and lncRNAs, thereby maintaining cellular RNA homeostasis.[25] Its central role in neurodegenerative diseases was first established in 2006, when two independent research groups simultaneously identified TDP-43 as the primary component of neuronal inclusions in patients with sporadic amyotrophic lateral sclerosis (sALS) and frontotemporal lobar degeneration

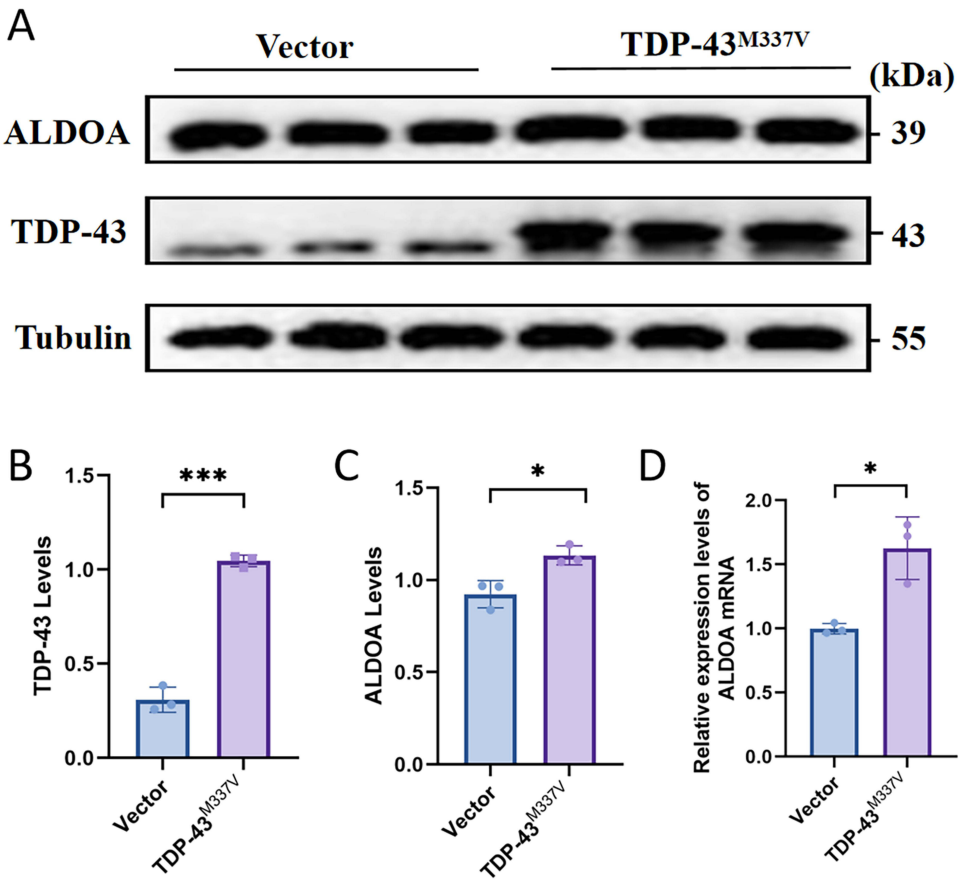

Figure 4 Expression of ALDOA is up-regulated in the TDP-43^{M337V} group. (**A**) Representative Western blot images of TDP-43 and ALDOA protein bands in each group. (**B** and **C**) Quantitative analysis of band intensities shown in (**A**). (**D**) mRNA expression levels of ALDOA in each group. Data were analyzed by unpaired t-test (n=3). *P < 0.05, ***P < 0.001 compared to the control group.

(FTLD).[26] Subsequent studies confirmed that the pathological aggregation of TDP-43 serves as a key biochemical hallmark of ALS.[27] In specific ALS subtypes, neuronal cytoplasmic inclusions formed by ubiquitinated and phosphorylated C-terminal TDP-43 fragments represent a characteristic neuropathological feature.[28,29] Notably, approximately 4% of familial ALS cases are directly linked to mutations in the TARDBP gene itself.[30] These pathogenic mutations (including M337V,[31] A382T,[32] G298S[33] and Q331K[34]) are predominantly clustered within the C-terminal glycine-rich domain of the TDP-43 protein. Among them, M337V, as one of the most frequent pathogenic mutations, plays a critical role in ALS pathogenesis: this mutation significantly enhances the abnormal aggregation propensity of TDP-43, disrupts its normal nucleocytoplasmic localization, impairs liquid-liquid phase separation equilibrium, and induces a cytotoxic gain-of-function in the cytoplasm. Consequently, these alterations compromise TDP-43's ability to regulate RNA metabolism, ultimately leading to motor neuron degeneration and driving the progression of ALS.[35]

ALDOA is a key enzyme in the glycolytic pathway. Its high expression enhances glycolytic flux primarily by elevating its catalytic efficiency, accelerating the conversion of glucose to pyruvate, thereby increasing lactate production and facilitating rapid ATP generation. Studies have demonstrated that ALDOA promotes disease progression in malignancies such as hepatocellular carcinoma (HCC) by enhancing glycolysis.[36] Furthermore, ALDOA has been implicated in neurodegenerative diseases. Research indicates that ALDOA and pyruvate kinase (PKM) are specifically upregulated in the cerebrospinal fluid (CSF) of Alzheimer's disease (AD) patients.[16] In sporadic Creutzfeldt-Jakob disease (sCJD), ALDOA expression is also specifically elevated and closely associated with prion protein (PrPSc) deposition and disease progression. The underlying mechanism may involve abnormal prion proteins interfering with the activity of ALDOA and other glycolytic enzymes, disrupting energy metabolism homeostasis in the brain.[37] Studies utilizing TDP-43 cellular models carrying familial ALS mutations (A315T, M337V and S379P), specifically a triple

https://doi.org/10.2147/DNND.S535954

mutant (3×-TDP-43) model, revealed that phosphorylated TDP-43 aggregates cause autophagy dysfunction and subsequently disrupt the expression of key glycolytic molecules, including ALDOA. This suggests that TDP-43 pathology may contribute to ALS pathogenesis by perturbing energy metabolism homeostasis.[38] However, the specific biological functions and molecular mechanisms of ALDOA in ALS remain incompletely elucidated. This study identified and experimentally validated an interaction between ALS biomarker protein TDP-43 and ALDOA, providing new directions for further exploration of ALDOA's role in ALS pathogenesis.

When ALDOA is highly expressed, it enhances glycolytic flux. The primary mechanism lies in the increased expression level of ALDOA directly elevating its catalytic efficiency, accelerating the conversion of glucose to pyruvate, which consequently leads to increased lactate production and rapid ATP generation. Under certain pathological conditions, the glycolytic process can be aberrantly activated and contribute to disease progression, as seen in cancers,[39] Alzheimer's disease,[40] and Parkinson's disease.[41] Notably, disrupted glycolysis has been demonstrated to participate in various pathological processes such as cellular apoptosis[42] and inflammatory responses,[43] suggesting that abnormalities in this pathway may represent a common mechanism underlying multiple neurological disorders.[44] In the pathogenesis of ALS, such coordinated metabolic mechanisms are disrupted, and metabolic dysregulation becomes a key factor driving disease progression. The interaction between TDP-43 and ALDOA and its alterations observed in this study may precisely represent one manifestation of glycolytic metabolic disruption in ALS.

This study integrated proteomics and molecular experiments by transfecting HEK293T cells with Flag-Vector, Flag-TDP-43, and Flag-TDP-43 ^{M337V} plasmids, respectively, to further investigate cellular mechanisms and related molecular targets. Based on the proteomics findings, we performed co-immunoprecipitation (co-IP) validation, which demonstrated that both wild-type TDP-43 and mutant TDP-43 ^{M337V} interact with the ALDOA protein. Furthermore, immunofluorescence assays confirmed the co-localization of ALDOA with both wild-type and mutant TDP-43 ^{M337V} in HEK293T cells. Subsequently, we examined ALDOA expression in the Vector group and the mutant TDP-43 M337V group. Both RT-qPCR and Western blot analyses revealed that compared to the Vector group, ALDOA mRNA and protein levels were elevated in the mutant TDP-43 ^{M337V} group, suggesting that TDP-43 mutation may upregulate ALDOA expression, thereby influencing the glycolytic pathway and contributing to the pathological process of ALS.

In summary, this study conducted an in-depth investigation of the proteome in cells transfected with ALS-associated wild-type and mutant TDP-43 plasmids, leading to the identification of ALDOA as an interacting partner. Differential expression levels of ALDOA were observed across various TDP-43 experimental groups. These findings establish a foundation for further exploration of the molecular mechanisms through which TDP-43-interacting protein ALDOA contributes to ALS pathogenesis. ALDOA and key proteins within its interactome may emerge as potential therapeutic targets for neurodegenerative diseases, suggesting that modulating the functions of these interacting proteins could offer novel strategic approaches for treatment.

Limitations of the Study

This study, through an in-depth investigation of the interaction between TDP-43 and ALDOA, reveals its potential role in the pathogenesis of ALS. The findings not only enhance the understanding of the pathophysiological processes of ALS but also provide a theoretical foundation for developing novel therapeutic strategies targeting this disease. However, this study has certain limitations, such as a relatively small sample size and the need for further optimization of experimental conditions. Future research should expand the sample size, delve deeper into the specific molecular mechanisms of the TDP-43-ALDOA interaction, and evaluate its feasibility and effectiveness as a therapeutic target. Moreover, utilizing preclinical models to further validate the translational potential of these findings could offer new hope for ALS patients.

Conclusion

This study confirms an interaction between TDP-43 and ALDOA, and demonstrates that the TDP-43 ^{M337V} mutation significantly promotes the upregulation of ALDOA expression. These results suggest that ALDOA, as a key glycolytic enzyme, may participate in TDP-43-mediated ALS pathogenesis by influencing cellular energy metabolism processes. The findings provide new experimental evidence for a deeper understanding of the molecular pathological mechanisms of ALS and also identify a potential target for therapeutic strategies aimed at intervening in metabolic pathways.

Funding

This study was supported by the Central Government Guidance Funds for Local Science and Technology Development (ZYYD2024ZY05) and the Xinjiang Medical University Young Top Talent Training Program (XYD2024Q08), National Natural Science Foundation of China (Grant No. 82171433), and Natural Science Foundation of Hunan Province of China (Grant No.2022JJ30918).

Disclosure

The authors report no conflicts of interest for this work.

References

1. Kiernan MC, Vucic S, Cheah BC, et al. Amyotrophic lateral sclerosis. *Lancet*. 2011;377(9769):942–955. PMID: 21296405. doi:10.1016/S0140-6736(10)61156-7
2. Verma A. Clinical manifestation and management of amyotrophic lateral sclerosis. In: Araki T, editor. *Amyotrophic Lateral Sclerosis*. Brisbane (AU): Exon Publications; 2021. Chapter 1. PMID: 34473441.
3. Mejzini R, Flynn LL, Pitout IL, et al. ALS genetics, mechanisms, and therapeutics: where are we now? *Front Neurosci*. 2019;13:1310. PMID: 31866818; PMCID: PMC6909825. doi:10.3389/fnins.2019.01310
4. Tzeplaeff L, Wilfling S, Requardt MV, et al. Current state and future directions in the therapy of ALS. *Cells*. 2023;12(11):1523. PMID: 37296644; PMCID: PMC10252394. doi:10.3390/cells12111523
5. Yang X, Ji Y, Wang W, et al. Amyotrophic lateral sclerosis: molecular mechanisms, biomarkers, and therapeutic strategies. *Antioxidants*. 2021;10(7):1012. PMID: 34202494; PMCID: PMC8300638. doi:10.3390/antiox10071012
6. Zhou C, Hardin EJ, Zimmer TS, et al. Neuroimmune signaling mediates astrocytic nucleocytoplasmic disruptions and stress granule formation associated with TDP-43 pathology. *Neurobiol Dis*. 2025;211:106939. PMID: 40339618; PMCID: PMC12240875. doi:10.1016/j.nbd.2025.106939
7. Zeng J, Luo C, Jiang Y, et al. Decoding TDP-43: the molecular chameleon of neurodegenerative diseases. *Acta Neuropathol Commun*. 2024;12(1):205. PMID: 39736783; PMCID: PMC11687198. doi:10.1186/s40478-024-01914-9
8. Kurashige T, Murao T, Kanaya Y, et al. Intramuscular nerve bundles reflect TDP-43 pathology in the medulla and spinal cord of ALS patients. *Neuropathol Appl Neurobiol*. 2025;51(2):e70016. PMID: 40192272; PMCID: PMC11974360. doi:10.1111/nan.70016
9. Chauhan S, Maan P, Panghal A. TDP-43 proteinopathies in ALS and FTLD: mechanistic insights and therapeutic approaches. *CNS Neurol Disord Drug Targets*. 2025;24. PMID: 40619651. doi:10.2174/0118715273374466250617085832
10. Horiuchi M, Watanabe S, Komine O, et al. ALS-linked mutant TDP-43 in oligodendrocytes induces oligodendrocyte damage and exacerbates motor dysfunction in mice. *Acta Neuropathol Commun*. 2024;12(1):184. PMID: 39605053; PMCID: PMC11603663. doi:10.1186/s40478-024-01893-x
11. Romano R, Del Fiore VS, Ruotolo G, et al. Lysosomal dysfunction in amyotrophic lateral sclerosis: a familial case linked to the p.G376D *TARDBP* mutation. *Int J Mol Sci*. 2025;26(7):2867. PMID: 40243477; PMCID: PMC11988578. doi:10.3390/ijms26072867
12. Verde EM, Secco V, Ghezzi A, et al. Molecular mechanisms of protein aggregation in ALS-FTD: focus on TDP-43 and cellular protective responses. *Cells*. 2025;14(10):680. PMID: 40422183; PMCID: PMC12109844. doi:10.3390/cells14100680
13. Sobanski T, Suraweera A, Burgess JT, et al. The fructose-bisphosphate, aldolase A (ALDOA), facilitates DNA-PKcs and ATM kinase activity to regulate DNA double-strand break repair. *Sci Rep*. 2023;13(1):15171. PMID: 37704669; PMCID: PMC10499815. doi:10.1038/s41598-023-41133-1
14. Zhao Y, Wang Y, Wu Y, et al. PKM2-mediated neuronal hyperglycolysis enhances the risk of Parkinson's disease in diabetic rats. *J Pharm Anal*. 2023;13(2):187–200. PMID: 36908857; PMCID: PMC9999299. doi:10.1016/j.jpha.2022.11.006
15. Li J, Chen L, Qin Q, et al. Upregulated hexokinase 2 expression induces the apoptosis of dopaminergic neurons by promoting lactate production in Parkinson's disease. *Neurobiol Dis*. 2022;163:105605. PMID: 34973450. doi:10.1016/j.nbd.2021.105605
16. de Geus MB, Leslie SN, Lam T, et al. Mass spectrometry in cerebrospinal fluid uncovers association of glycolysis biomarkers with Alzheimer's disease in a large clinical sample. *Sci Rep*. 2023;13(1):22406. PMID: 38104170; PMCID: PMC10725469. doi:10.1038/s41598-023-49440-3
17. Rozanova S, Barkovits K, Nikolov M, et al. Quantitative mass spectrometry-based proteomics: an overview. *Methods Mol Biol*. 2021;2228:85–116. PMID: 33950486. doi:10.1007/978-1-0716-1024-4_8
18. Karayel O, Virreira Winter S, Padmanabhan S, et al. Proteome profiling of cerebrospinal fluid reveals biomarker candidates for Parkinson's disease. *Cell Rep Med*. 2022;3(6):100661. PMID: 35732154; PMCID: PMC9245058. doi:10.1016/j.xcrm.2022.100661
19. Di Domenico F, Zuliani I, Tramutola A. Shining a light on defective autophagy by proteomics approaches: implications for neurodegenerative illnesses. *Expert Rev Proteomics*. 2019;16(11–12):951–964. PMID: 31709850. doi:10.1080/14789450.2019.1691919
20. Goutman SA, Hardiman O, Al-Chalabi A, et al. Emerging insights into the complex genetics and pathophysiology of amyotrophic lateral sclerosis. *Lancet Neurol*. 2022;21(5):465–479. doi:10.1016/S1474-4422(21)00414-2
21. Ho PC, Hsieh TC, Tsai KJ. TDP-43 proteinopathy in frontotemporal lobar degeneration and amyotrophic lateral sclerosis: from pathomechanisms to therapeutic strategies. *Ageing Res Rev*. 2024;100:102441. doi:10.1016/j.arr.2024.102441
22. Korobeynikov VA, Lyashchenko AK, Blanco-Redondo B, Jafar-Nejad P, Shneider NA. Antisense oligonucleotide silencing of FUS expression as a therapeutic approach in amyotrophic lateral sclerosis. *Nat Med*. 2022;28(1):104–116. doi:10.1038/s41591-021-01615-z
23. Modafferi S, Farina S, Esposito F, et al. DNA damage response defects induced by the formation of TDP-43 and mutant FUS cytoplasmic inclusions and their pharmacological rescue. *Cell Death Differ*. 2025. doi:10.1038/s41418-025-01530-7
24. Piol D, Robberechts T, Da Cruz S. Lost in local translation: TDP-43 and FUS in axonal/neuromuscular junction maintenance and dysregulation in amyotrophic lateral sclerosis. *Neuron*. 2023;111(9):1355–1380. doi:10.1016/j.neuron.2023.02.028
25. Cheng F, Chapman T, Zhang S, et al. Understanding age-related pathologic changes in TDP-43 functions and the consequence on RNA splicing and signalling in health and disease[J]. *Ageing Res Rev*. 2024;96:102246. doi:10.1016/j.arr.2024.102246
26. Arai T, Hasegawa M, Akiyama H, et al. TDP-43 is a component of ubiquitin-positive tau-negative inclusions in frontotemporal lobar degeneration and amyotrophic lateral sclerosis. *Biochem Biophys Res Commun*. 2006;351(3):602–611. PMID: 17084815. doi:10.1016/j.bbrc.2006.10.093

27. San Gil R, Pascovici D, Venturato J, et al. A transient protein folding response targets aggregation in the early phase of TDP-43-mediated neurodegeneration. *Nat Commun*. 2024;15(1):1508. doi:10.1038/s41467-024-45646-9
28. Lee YC, Huang WC, Lin JH, et al. Znf179 E3 ligase-mediated TDP-43 polyubiquitination is involved in TDP-43- ubiquitinated inclusions (UBI) (+)-related neurodegenerative pathology. *J Biomed Sci*. 2018;25(1):76. doi:10.1186/s12929-018-0479-4
29. Ko VI, Ong K, Kwon DY, et al. CK1δ/ε-mediated TDP-43 phosphorylation contributes to early motor neuron disease toxicity in amyotrophic lateral sclerosis. *Acta Neuropathol Commun*. 2024;12(1):187. doi:10.1186/s40478-024-01902-z
30. Mackenzie IR, Rademakers R, Neumann M. TDP-43 and FUS in amyotrophic lateral sclerosis and frontotemporal dementia. *Lancet Neurol*. 2010;9 (10):995–1007. PMID: 20864052. doi:10.1016/S1474-4422(10)70195-2
31. Gordon D, Dafinca R, Scaber J, et al. Single-copy expression of an amyotrophic lateral sclerosis-linked TDP-43 mutation (M337V) in BAC transgenic mice leads to altered stress granule dynamics and progressive motor dysfunction. *Neurobiol Dis*. 2019;121:148–162. doi:10.1016/j.nbd.2018.09.024
32. Zanini G, Selleri V, Nasi M, et al. Mitochondrial and endoplasmic Reticulum alterations in a case of amyotrophic lateral sclerosis caused by TDP-43 A382T mutation. *Int J Mol Sci*. 2022;23(19):11881. doi:10.3390/ijms231911881
33. Buck E, Oeckl P, Grozdanov V, et al. Increased NF-L levels in the TDP-43G298S ALS mouse model resemble NF-L levels in ALS patients. *Acta Neuropathol*. 2022;144(1):161–164. doi:10.1007/s00401-022-02436-1
34. Lee JD, Levin SC, Willis EF, Li R, Woodruff TM, Noakes PG. Complement components are upregulated and correlate with disease progression in the TDP-43Q331K mouse model of amyotrophic lateral sclerosis. *J Neuroinflammation*. 2018;15(1):171. doi:10.1186/s12974-018-1217-2
35. Zeng J, Tang Y, Dong X, Li F, Wei G Influence of ALS-linked M337V mutation on the conformational ensembles of TDP-43321-340 peptide monomer and dimer. *Proteins*. 2024;92(9):1059–1069. doi:10.1002/prot.26482
36. Meng W, Lu X, Wang G, et al. ZNF692 drives malignant development of hepatocellular carcinoma cells by promoting ALDOA-dependent glycolysis[J]. *Funct Integr Genomics*. 2024;24(2):53. doi:10.1007/s10142-024-01326-x
37. Gawinecka J, Dieks J, Asif AR, et al. Codon 129 polymorphism specific cerebrospinal fluid proteome pattern in sporadic Creutzfeldt-Jakob disease and the implication of glycolytic enzymes in prion-induced pathology. *J Proteome Res*. 2010;9(11):5646–5657. doi:10.1021/pr1004604
38. Dopler MB, Abeer MI, Arezoumandan S, et al. A cellular model of TDP −43 induces phosphorylated TDP −43 aggregation with distinct changes in solubility and autophagy dysregulation. *FEBS J*. 2025;292(18):4870–4897. PMID: 39887552; PMCID: PMC12310990. doi:10.1111/febs.17413
39. Paul S, Ghosh S, Kumar S. Tumor glycolysis, an essential sweet tooth of tumor cells[J]. *Semin Cancer Biol*. 2022;86(Pt 3).
40. Zhang Y, Yang X, Zhuang J, et al. β-Amyloid activates reactive astrocytes by enhancing glycolysis of astrocytes[J]. *Mol Biol Rep*. 2022;49 (6):4699–4707. doi:10.1007/s11033-022-07319-y
41. Zhao Y, Wang Y, Wu Y, et al. PKM2-mediated neuronal hyperglycolysis enhances the risk of Parkinson's disease in diabetic rats[J]. *J Pharm Anal*. 2023;13(2):187–200.
42. Gunasangkaran G, Muthukrishnan S, Ravi AK, et al. Targeting the lncRNA RBM5-AS1/GCN5 axis under fasting conditions reprograms Glycolysis and induces apoptosis in ovarian cancer cells. *Mol Biol Rep*. 2025;52(1):691. doi:10.1007/s11033-025-10800-z. PMID: 40632300..
43. Liu Y, Han C, Guo L, et al. Deer antler uridine regulates glycolysis in microglia via HSP90/HIF-1α to improve cognitive impairment in Alzheimer's disease mice. *CNS Neurosci Ther*. 2025;31(5). doi:10.1111/cns.70416
44. Gao R, Gao Y, Su W, Wang R. Decoding microglial polarization and metabolic reprogramming in neurodegenerative diseases: implications for disease progression and therapy. *Aging Dis*. 2025. PMID: 40072374. doi:10.14336/AD.2024.1629